Dentomaxillofacial Radiology (2019) 48, 20170471

birpublications.org/dmfr

RESEARCH ARTICLE

Intensity of artefacts in cone beam CT examinations caused by titanium and glass fibre-reinforced composite implants

[1,2,3]Niina Kuusisto, [1,3,4,5,6]Sisko Huumonen, [7,8,9]Antti Kotiaho, [7,8,9]Marianne Haapea, [10]Jami Rekola and [2]Pekka Vallittu

[1]Department of Oral Pathology and Radiology, Institute of Dentistry, University of Turku, Turku, Finland; [2]Department of Biomaterials Science and Turku Clinical Biomaterials Centre – TCBC, Institute of Dentistry and BioCity, University of Turku and City of Turku, Welfare Division, Turku, Finland; [3]Department of Diagnostic Imaging, Turku University Hospital, Turku, Finland; [4]Department of Oral Radiology, Institute of Dentistry, University of Eastern Finland, Kuopio, Finland; [5]Department of Oral and Maxillofacial Surgery, Kuopio University Hospital, Unit of Oral HealthSciences, Kuopio, Finland; [6]Department of Oral Radiology, Institute of Dentistry, University of Oulu, Oulu, Finland; [7]Department of Diagnostic Radiology, Oulu University Hospital, Oulu, Finland; [8]Department of Physics and Technology, Research Unit of Medical Imaging, Physics and Technology, University of Oulu, Oulu, Finland; [9]Medical Research Center, Organisation of Oulu University Hospital and University of Oulu, Oulu, Finland; [10]Department of Otorhinolaryngology, Turku University Hospital, Turku, Finland

Objectives: The aim was to compare titanium and glass fibre-reinforced composite (FRC) orbital floor implants using cone beam CT (CBCT). FRC implants are nonmetallic and these implants have not been analysed in CBCT images before. The purpose of this study is to compare the artefact formation of the titanium and the FRC orbital floor implants in CBCT images.
Methods: One commercially pure titanium and one S-glass FRC with bioactive glass particles implant were imaged with CBCT using the same imaging values (80 kV, 1 mA, FOV 60 × 60 mm). CBCT images were analysed in axial slices from three areas to determine the magnitude of the artefacts in the vicinity of the implants. Quantified results based on the gray values of images were analysed using analysis-of-variance.
Results: Compared to the reference the gray values of the titanium implant are more negative in every region of interest in all slices ($p < 0.05$) whereas the gray values of the FRC implant differ statistically significantly in less than half of the examined areas.
Conclusions: The titanium implant caused artefacts in all of the analysed CBCT slices. Compared to the reference the gray values of the FRC implant changed only slightly and this feature enables to use wider imaging options postoperatively.
Dentomaxillofacial Radiology (2019) **48**, 20170471. doi: 10.1259/dmfr.20170471

Cite this article as: Kuusisto N, Huumonen S, Kotiaho A, Haapea M, Rekola J, Vallittu P. Intensity of artefacts in cone beam CT examinations caused by titanium and glass fibre-reinforced composite implants. *Dentomaxillofac Radiol* 2019; **48**: 20170471.

Keywords: cone-beam computed tomography; artefact; orbital implants

Introduction

Diagnosis and treatment planning in the maxillofacial area often requires three-dimensional imaging because of the complex anatomy of bone structures. The orbital area especially, consists of complex and thin bone structures. If orbital floor fractures are suspected, the clinical diagnosis has to be confirmed by imaging, particularly if an operation is being considered. Cone beam CT (CBCT) is widely used to diagnose fractures and to control bone growth, resorption, and infections postoperatively.[1–3] However, CBCT technique can cause several artefacts because of the technique itself and the properties of the examined object. An artefact is a distortion in the image which is induced by differences among the

Correspondence to: Ms Niina Kuusisto, E-mail: niinakuusisto@ymail.com
Received 15 December 2017; revised 16 July 2018; accepted 01 August 2018

assumptions in image reconstruction and the physical imaging process. In the worst cases, artefacts can complicate the diagnosis. Artefacts occur when CBCT is used in regions with dense objects, mostly metallic materials. Metal artefacts are basically dependent on the atomic weight of the metal, and the size and the thickness of the implant.[4–6] Beam hardening artefacts which are seen as dark streaks are the most common when imaging metallic materials.[7]

Clinically relevant defects of the orbital floor are usually reconstructed with implants to maintain the volume of the orbit and to avoid sequelae such as enophthalmos, diplopia, limited ocular movement and altered sensory function of the infraorbital nerve.[8–11] The implant material should be biocompatible, as strong as necessary, ductile, nonmagnetic and with low thermal conductivity. In addition, postoperative imaging requires that the implant material does not impair the image quality with artefacts. Commercially pure titanium and titanium alloys are widely used as implant materials because of their minimal infection risk.[12–14] Titanium has also been shown to be more accurate in anatomical reconstructions than autogenous calvarial bone, for example.[14] However, titanium causes artefacts in CBCT.[4–6]

Biomaterial science has studied synthetic fibre-reinforced composites (FRC) as a substitutive material for bones and teeth. These are non-metallic composite materials, which are based on co-polymer matrices of polymethyl methacrylate or bisphenol-A-dimethacrylate (Bis-GMA) and triethylenecoldimethacrylate (TEGDMA) strengthened with glass fibres. These composite materials are used in dental restorations.[15,16] The orbital floor FRC implant used in this study consists of composite and glass fibre network layers. Bioactive glass granules are placed in the middle of the implant to facilitate intergration into the bone. The porous network structure allows bone-ingrowth, fluid exhance, cell migration, vascularisation and tissue ingrowth, while it also maintains the strength.[17,18] The biocompability of the FRC implants are already verified in animal models and in cranial bone reconstruction operations on patients since 2007.[19–24]

Because composite based implants are nonmetallic, they are assumed to be able to be imaged with CBCT without artefacts. The radiological properties of the FRC orbital floor implants in CBCT imaging have not been studied before. The aim of this study is to compare the titanium and the FRC implants of the orbital floor in CBCT images focusing on the prospective artefacts which are caused by these implants.

Methods and materials

One perforated preformed commercially pure titanium plate (size: large 35 × 40 × 0.4 mm, MatrixORBITAL, DePuy Synthe, Oberdorf, Switzerland) and one standard size glass FRC orbital floor implant (size: large 24 × 29 mm, Glace, Skulle Implants Corporation, Turku, Finland) were imaged separately with CBCT (3D Accuitomo 170, J Morita, Kyoto, Japan) using the same imaging values (80 kV, 1 mA, FOV 60 × 60 mm). The FRC implant's shape followed the titanium plate's shape. Titanium plate has been laser scanned and the 3D data is used to fabricate a special mold for preparing the FRC implants. The thickness of the margins of the FRC implant is 0.5 mm and the center of the implant, the area of bioactive glass, has a thickness of 1.5 mm. The implant surface is mesh-like with opening size of an average of 250 × 600 micrometers (Figure 1).

Figure 1 The FRC (left) and the titanium implant of the orbital floor. FRC, fibre-reinforced composite.

The FRC implant is perforated S-glass (nominal composition in wt%: SiO_2 62–65; Al_2O_3 20–25; MgO 10–15; B_2O_3 0–1.2; Na_2O 0–1.1; Fe_2O_3 0.2) in a dimethacrylate polymer matrix and bioactive glass particles (S53P4; nominal composition in wt. %: Na_2O 24.5; CaO 24.5; SiO_2 45; P_2O_5 6). The average particle size of the bioactive glass in the FRC implant is 400 µm. Glass fibre loading in the dimetacrylate matrix is ca. 60 vol%.

Both implants were supported with the same natural human skull (The Department of Oral Pathology and Radiology, Institute of Dentistry, University of Turku, Finland) which is intended for teaching and research. In addition, the skull was imaged without the implants using the same values for reference. The implants were placed on the orbital floor of the skull without screws (Figure 2). On patients the titanium plates are usually placed without screw fixation, although in complicated fractures anterior screw fixation is sometimes needed.

CBCT images of the orbital floor implants and the skull were analysed using an in-house script written with Matlab (Matlab R2016b, The MathWorks, Natick, MA). The FRC and the titanium images were registered with the reference image in 3D, so that the skull structures would be in the same place for the analysis. Three region of interest (ROI) were used in nine consecutive transversal slices to evaluate the amount of artefact caused by the implants. The parallelogram shaped

Figure 2 The position of the FRC implant on the orbital floor of the skull. FRC, fibre-reinforced composite.

ROIs and the number of the slices were chosen based on the visible artefacts of the titanium implant. The size and location of the ROIs were chosen by a specialising radiologist, a radiologist with 17 years of experience and a physicist. In different slices artefact lines were recognised to change their places a little and therefore ROIs were chosen so that the artefact lines would be covered throughout the nine slices. ROIs were placed on anterior (ROI 1), lateral (ROI 2) and medial (ROI 3) side of the orbital floor and the ROI areas (base x height) were 2697 (3.8 × 13.8 mm), 2880 (14.4 × 3.9 mm) and 1224 (13.5 × 1.4 mm) pixels respectively (Figure 3). The mean and standard deviation of gray values on each ROI were obtained.

The mean values between the reference and the FRC and titanium ROIs were compared using one-way analysis of variance (ANOVA). The differences between the FRC and the reference and between the titanium and the reference were tested using Tukey's test (equal variances between the groups) or Games-Howell's test (un-equal variances between the groups). The Benjamini-Hochberg method was used to correct for multiple comparisons separately for ROIs, *i.e.* for 18 comparisons in each ROI. *p*-values less than 0.05 were considered statistically significant. The analyses were conducted using SPSS Statistics v.23, IBM, corporation, Armonk, NY.

Results

Table 1 presents the mean and the standard deviations (SD) of the gray values on each ROI of the nine slices. The mean gray values of the titanium and the reference differ on average 19.4 units in ROI 1, 33.8 units in ROI 2 and 79.5 units in ROI 3. The gray values of the titanium are more negative than the gray values of the reference in every ROI in all slices ($p < 0.05$). The mean gray values of the FRC and the reference differ on average 3.5 units in ROI 1, 8.5 units in ROI 2 and 10.6 units in ROI 3. The gray values of the FRC and the reference differ statistically significantly in three slices in ROI 1 (slices 1 to 3 $p < 0.05$), four slices in ROI 2 (slices 1 to 3 and slice 8 $p < 0.05$), and four slices in ROI 3 (slices 2, 3, 6 and 8 $p < 0.05$). The average standard deviation of the gray values of the reference is 25.2, the FRC 23.0 and the titanium 39.1 in ROI 1. The corresponding standard deviations are 51.9, 50.3 and 83.8 in ROI 2 and 85.5, 79.6, 131.2 in ROI 3.

Discussion

The main reason to investigate the artefacts in CBCT images caused by artificial materials like titanium and zirconium dioxide is to learn to avoid them. Presently, it is known that artefacts can not be removed entirely when metallic implants are used, and, that using the image sofwares of the imaging systems to eliminate artefacts may delete the diagnostically important image data. There are various technical and computational solutions to weaken the artefacts in order to improve the image quality. Artefacts can be reduced with special metal correction algorithms during image

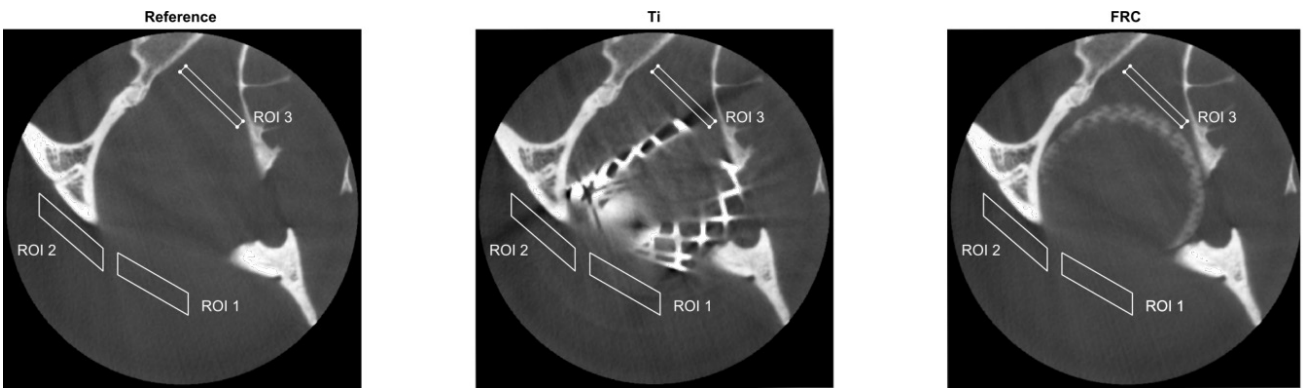

Figure 3 The ROIs in the transversal plane at slice 3 from the reference, titanium and FRC. FRC, fibre-reinforced composite; ROI, region of interest.

Table 1 The results of ANOVA tests with mean and standard deviations of gray values of different regions of interest (ROIs) from different measurements

	Ref Mean (SD)	*FRC Mean (SD)*	*Ti Mean (SD)*	*P1 FRC vs Ref*	*P2 Ti vs Ref*
ROI 1					
Slice 1	−137.9 (36.7)	−152.3 (35.3)	−150.9 (37.7)	<0.001	<0.001
Slice 2	−131.2 (26.9)	−139.0 (24.2)	−178.5 (67.1)	<0.001	<0.001
Slice 3	−124.9 (26.6)	−130.3 (23.5)	−136.9 (73.1)	<0.001	<0.001
Slice 4	−116.7 (22.9)	−117.4 (20.6)	−138.4 (38.9)	0.502	<0.001
Slice 5	−113.4 (22.5)	−113.1 (20.2)	−129.2 (33.4)	0.764	<0.001
Slice 6	−107.6 (23.0)	−108.0 (20.4)	−123.5 (30.5)	0.668	<0.001
Slice 7	−102.7 (22.1)	−103.8 (22.3)	−120.9 (26.6)	0.153	<0.001
Slice 8	−99.7 (22.5)	−100.7 (20.6)	−117.1 (22.9)	0.190	<0.001
Slice 9	−96.4 (23.3)	−96.8 (20.2)	−109.9 (21.5)	0.740	<0.001
ROI 2					
Slice 1	−250.7 (57.8)	−267.7 (56.5)	−264.0 (58.6)	<0.001[a]	<0.001[a]
Slice 2	−232.7 (55.1)	−243.4 (52.4)	−278.4 (102.7)	<0.001	<0.001
Slice 3	−212.0 (44.5)	−220.4 (47.3)	−277.4 (97.9)	<0.001	<0.001
Slice 4	−176.4 (46.2)	−195.3 (39.6)	−238.9 (114.2)	0.215	<0.001
Slice 5	−165.5 (51.5)	−178.7 (45.9)	−217.0 (108.5)	0.181	<0.001
Slice 6	−165.5 (51.5)	−167.9 (51.1)	−191.9 (90.1)	0.196	<0.001
Slice 7	−159.2 (52.5)	−160.7 (52.9)	−176.6 (69.8)	0.559	<0.001
Slice 8	−155.7 (54.8)	−157.5 (54.0)	−167.6 (56.4)	<0.001[a]	<0.001[a]
Slice 9	−151.1 (52.8)	−153.8 (53.2)	−160.8 (56.0)	0.152	<0.001
ROI 3					
Slice 1	252.3 (448.9)	214.9 (422.1)	150.3 (365.4)	0.086	<0.001
Slice 2	−10.4 (150.5)	−33.9 (137.9)	−156.0 (83.7)	<0.001	<0.001
Slice 3	−79.9 (32.4)	−102.7 (31.6)	−182.1 (116.4)	<0.001	<0.001
Slice 4	−81.8 (31.0)	−81.0 (30.3)	−144.5 (146.8)	0.775	<0.001
Slice 5	−73.6 (21.8)	−71.9 (21,2)	−141.5 (111.9)	0.130	<0.001
Slice 6	−78.4 (19.4)	−80.6 (18.5)	−141.8 (116.1)	0.011	<0.001
Slice 7	−79.4 (19.9)	−80.1 (18.5)	−148.7 (108.2)	0.633	<0.001
Slice 8	−79.5 (24.0)	−83.7 (20.0)	−140.0 (74.8)	<0.001	<0.001
Slice 9	−74.9 (21.2)	−76.6 (16.5)	−116.5 (57.9)	0.087	<0.001

FRC, fibre-reinforced composite group; Ref, reference group; SD, standard deviation; Ti, titanium group.
P1 = significance from Tukey's or Games-Howell's test ([a]Tukey's HSD) FRC *vs* reference.
P2 = significance from Tukey's or Games-Howell's test ([a] Tukey's HSD) Ti *vs* reference.
All the significant (<0.05) *p*-values remained significant after Benjamini-Hochberg's procedure.

reconstruction. Peltola et al for example, noticed that if a streak artefact occurs, it is usually safer for it to remain recognisable than to fill the image with factitious data to make it smoother. In addition, the non-iterative CBCT with or without a metal reduction algorithm for post-operative facial imaging is not recommended.[25]

The implants of this study were standard-sized implants which were not customised or modified for this study. The size and the shape of them were as similar as possible which were available for this study. However, the possibility to customise the implant material is important. Titanium orbital floor implants are sometimes customised pre- or peri-operatively to facilitate the best possible anatomical reconstruction. FRC implants can also be customised pre-operatively before the polymerisation of the implant material.[19,26] During examination both the titanium and the FRC implant were fitted in the same anatomical position on the orbital floor of the skull. The implants were positioned on the orbital floor to emulate a real surgical situation. Because the implants were not modified for this study and they were not exactly the same size the borders of the implants did not fit perfectly and similarly on the orbital floor. This may have an influence on the measured gray values.

The use of a real skull helped to target the artefacts in CBCT slices. The bony structure of the skull gives a backround that is as realistic as possible for artefacts. However, it is important to consider that the thickness of the bone around the orbital floor alternates because of the complex anatomy and this may affect on the measured gray values, as well. In addition, metal artefacts are enhanced especially in the soft-tissue region because of the lower contrast of the soft-tissue in CBCT images.[27] This study does not simulate the *in vivo* situation perfectly because of the lacking soft tissues and

therefore we can not investigate whether the artefacts weaken the image quality in the soft tissue areas or thin bone structure areas.

This study focused on nine axial slices and three different ROIs which were chosen on the basis of the artefact formation that could be obviously seen by the radiologists of this study. Compared to the reference the gray values of the titanium implant are more negative in every ROI in all slices. Since the more negative gray values of the titanium implant are considered as artefact formation the titanium implant is presumed to cause more artefacts than the FRC implant. Because this image analysis does not represent the entire imaged area it is possible to see more artefact formation around the titanium implant outside the determined ROIs. After all, artefacts are basically expected in the transversal direction in which the CBCT radiation collides the object. Therefore the artefacts caused by the titanium orbital floor implant are not excepted in the denture area, for example.

Compared to the reference the gray values of the FRC implant differ statistically significantly in less than half of the slices of the ROIs. These results imply that the FRC implant did not demonstrate obvious artefacts. Due to the elemental composition of glass fibres used in the FRC implant, it has a radiopacity close to that of cortical bone. The FRC implant is assumed to be radiologically bone-like, though, it can be recognised in CBCT images. Besides radiography, this property could also be beneficial in MRI and in radiation therapy. Titanium, although it is a non-magnetising metal, has proved to be problematic in MRI.[28–33]

The radiological properties of other non-metallic implant material, carbon-fibre-reinforced composite, has been investigated by Hak et al. As a result carbon-fibre-reinforced composite did not cause artefacts.[34] As mentioned before, the artefact formation is dependent on the atomic weight of the material. In addition to metals, if composite material includes radio-opaque filling enough, it is possible that artefact formation emerges in CBCT images.[35] This study does not exclude that a FRC implant thick enough could cause aretafacts in CBCT images. More studies of imaging different kind of FRC implants with CBCT are needed.

This study focuses on the differences of the titanium and the FRC orbital floor implants in CBCT images. The results of this study imply that the FRC implants would be a good choice for titanium and other metal implants in the orbital area when CBCT imaging is used. The possible complications of the implant, such as infection, resorption and possible changes of the position of the implant, has to be controlled postoperatively. The radiological features of the FRC implant enables clinicians to use wider imaging options and helps to diagnose these complications unhesitatingly and quicker. Consequently, it is clinically relevant that the FRC implants do not cause artefacts, and equally relevant that they are visible in CBCT images.

References

1. Roman R, Hedeşiu M, Fildan F, Ileşan R, Mitea D, Dinu C, et al. The use of reformatted Cone Beam CT images in assessing mid-face trauma, with a focus on the orbital floor fractures. *Clujul Med* 2016; **89**: 519–24. doi: https://doi.org/10.15386/cjmed-601
2. Johari M, Ghavimi MA, Mahmoudian H, Javadrashid R, Mirakhor Samani S, Fouladi DF. A comparable study of the diagnostic performance of orbital ultrasonography and CBCT in patients with suspected orbital floor fractures. *Dentomaxillofac Radiol* 2016; **45**: 20150311. doi: https://doi.org/10.1259/dmfr.20150311
3. Drage NA, Sivarajasingam V. The use of cone beam computed tomography in the management of isolated orbital floor fractures. *Br J Oral Maxillofac Surg* 2009; **47**: 65–6. doi: https://doi.org/10.1016/j.bjoms.2008.05.005
4. Benic GI, Sancho-Puchades M, Jung RE, Deyhle H, Hämmerle CH. In vitro assessment of artifacts induced by titanium dental implants in cone beam computed tomography. *Clin Oral Implants Res* 2013; **24**: 378–83. doi: https://doi.org/10.1111/clr.12048
5. Pauwels R, Stamatakis H, Bosmans H, Bogaerts R, Jacobs R, Horner K, et al. Quantification of metal artifacts on cone beam computed tomography images. *Clin Oral Implants Res* 2013; **24**: 94–9. doi: https://doi.org/10.1111/j.1600-0501.2011.02382.x
6. Schulze RK, Berndt D, d'Hoedt B, d'Hoedt B. On cone-beam computed tomography artifacts induced by titanium implants. *Clin Oral Implants Res* 2010; **21**: 100–7. doi: https://doi.org/10.1111/j.1600-0501.2009.01817.x
7. De Man B, Nuyts J, Dupont P, Marchal G, Suetens P. Metal streak artifacts in X-ray computed tomography: a simulation study. *IEEE Trans Nucl Sci* 1999; **46**: 691–6. doi: https://doi.org/10.1109/23.775600
8. Gosse EM, Ferguson AW, Lymburn EG, Gilmour C, MacEwen CJ. Blow-out fractures: patterns of ocular motility and effect of surgical repair. *Br J Oral Maxillofac Surg* 2010; **48**: 40–3. doi: https://doi.org/10.1016/j.bjoms.2009.04.028
9. Stoor P, Suomalainen A, Lindqvist C, Mesimäki K, Danielsson D, Westermark A, et al. Rapid prototyped patient specific implants for reconstruction of orbital wall defects. *J Craniomaxillofac Surg* 2014; **42**: 1644–9. doi: https://doi.org/10.1016/j.jcms.2014.05.006
10. Salentijn EG, van den Bergh B, Forouzanfar T. A ten-year analysis of midfacial fractures. *J Craniomaxillofac Surg* 2014; **42**: 1717–22.
11. Wang S, Xiao J, Liu L, Lin Y, Li X, Tang W, et al. Orbital floor reconstruction: a retrospective study of 21 cases. *Oral Surg Oral Med Oral Pathol Oral Radiol Endod* 2008; **106**: 324–30. doi: https://doi.org/10.1016/j.tripleo.2007.12.022
12. Gear AJ, Lokeh A, Aldridge JH, Migliori MR, Benjamin CI, Schubert W. Safety of titanium mesh for orbital reconstruction. *Ann Plast Surg* 2002; **48**: 1–9. doi: https://doi.org/10.1097/00000637-200201000-00001
13. Sugar AW, Kuriakose M, Walshaw ND. Titanium mesh in orbital wall reconstruction. *Int J Oral Maxillofac Surg* 1992; **21**: 140–4. doi: https://doi.org/10.1016/S0901-5027(05)80780-5
14. Ellis E, Tan Y. Assessment of internal orbital reconstructions for pure blowout fractures: cranial bone grafts versus titanium mesh. *J Oral Maxillofac Surg* 2003; **61**: 442. doi: https://doi.org/10.1053/joms.2003.50085
15. Vallittu PK. Flexural properties of acrylic resin polymers reinforced with unidirectional and woven glass fibers. *J Prosthet Dent*

1999; **81**: 318–26. doi: https://doi.org/10.1016/S0022-3913(99)70276-3
16. Vallittu PK, Sevelius C. Resin-bonded, glass fiber-reinforced composite fixed partial dentures: a clinical study. *J Prosthet Dent* 2000; **84**: 413–8. doi: https://doi.org/10.1067/mpr.2000.109782
17. Jones JR, Atwood RC, Poologasundarampillai G, Yue S, Lee PD. Quantifying the 3D macrostructure of tissue scaffolds. *J Mater Sci Mater Med* 2009; **20**: 463–71. doi: https://doi.org/10.1007/s10856-008-3597-9
18. Ylä-Soininmäki A, Moritz N, Lassila LV, Peltola M, Aro HT, Vallittu PK. Characterization of porous glass fiber-reinforced composite (FRC) implant structures: porosity and mechanical properties. *J Mater Sci Mater Med* 2013; **24**: 2683–93. doi: https://doi.org/10.1007/s10856-013-5023-1
19. Tuusa SM, Peltola MJ, Tirri T, Puska MA, Röyttä M, Aho H, et al. Reconstructioin of critical size calvarial bone defects in rabbits with glass-fibre-reinforced composite with bioactive glass granule coating. *J Biomed Mater Res B Appl Biomater* 2007; **82**: 149–55.
20. Aitasalo KM, Piitulainen JM, Rekola J, Vallittu PK. Craniofacial bone reconstruction with bioactive fiber-reinforced composite implant. *Head Neck* 2014; **36**: 722–8. doi: https://doi.org/10.1002/hed.23370
21. Posti JP, Piitulainen JM, Hupa L, Fagerlund S, Frantzén J, Aitasalo KMJ, et al. A glass fiber-reinforced composite – bioactive glass cranioplasty implant. A case study of an early development stage implant removed due to a late infection. *J Mech Behav Biomed Mater* 2016; **55**: 191–200.
22. Piitulainen JM, Kauko T, Aitasalo KM, Vuorinen V, Vallittu PK, Posti JP. Outcomes of cranioplasty with synthetic materials and autologous bone grafts. *World Neurosurg* 2015; **83**: 708–14. doi: https://doi.org/10.1016/j.wneu.2015.01.014
23. Piitulainen JM, Posti JP, Aitasalo KM, Vuorinen V, Vallittu PK, Serlo W. Pediatric cranial defect reconstruction using bioactive fiber reinforced composite implant: Early outcomes. *Acta Neurochir* 2015; **157**: 681–7.
24. Vallittu PK. Bioactive glass-containing cranial implants: an overview. *J Mater Sci* 2017; **52**: 8772–84. doi: https://doi.org/10.1007/s10853-017-0888-x
25. Peltola EM, Mäkelä T, Haapamäki V, Suomalainen A, Leikola J, Koskinen SK, et al. CT of facial fracture fixation: an experimental study of artefact reducing methods. *Dentomaxillofac Radiol* 2017; **46**: 20160261. doi: https://doi.org/10.1259/dmfr.20160261
26. Mustafa SF, Evans PL, Bocca A, Patton DW, Sugar AW, Baxter PW. Customized titanium reconstruction of post-traumatic orbital wall defects: a review of 22 cases. *Int J Oral Maxillofac Surg* 2011; **40**: 1357–62. doi: https://doi.org/10.1016/j.ijom.2011.04.020
27. Zhang Y, Zhang L, Zhu XR, Lee AK, Chambers M, Dong L. Reducing metal artifacts in cone-beam CT images by preprocessing projection data. *Int J Radiat Oncol Biol Phys* 2007; **67**: 924–32. doi: https://doi.org/10.1016/j.ijrobp.2006.09.045
28. Abbaszadeh K, Heffez LB, Mafee MF. Effect of interference of metallic objects on interpretation of T1-weighted magnetic resonance images in the maxillofacial region. *Oral Surg Oral Med Oral Pathol Oral Radiol Endod* 2000; **89**: 759–65. doi: https://doi.org/10.1067/moe.2000.105942
29. Eggers G, Rieker M, Kress B, Fiebach J, Dickhaus H, Hassfeld S. Artefacts in magnetic resonance imaging caused by dental material. *MAGMA* 2005; **18**: 103–11. doi: https://doi.org/10.1007/s10334-005-0101-0
30. Smeets R, Schöllchen M, Gauer T, Aarabi G, Assaf AT, Rendenbach C, et al. Artefacts in multimodal imaging of titanium, zirconium and binary titanium-zirconium alloy dental implants: an in vitro study. *Dentomaxillofac Radiol* 2017; **46**: 20160267. doi: https://doi.org/10.1259/dmfr.20160267
31. Lu W, Pauly KB, Gold GE, Pauly JM, Hargreaves BA. Slice encoding for metal artifact correction with noise reduction. *Magn Reson Med* 2011; **65**: 1352–7. doi: https://doi.org/10.1002/mrm.22796
32. Lu W, Pauly KB, Gold GE, Pauly JM, Hargreaves BA. SEMAC: slice encoding for metal artifact correction in MRI. *Magn Reson Med* 2009; **62**: 66–76. doi: https://doi.org/10.1002/mrm.21967
33. Cortes AR, Abdala-Junior R, Weber M, Arita ES, Ackerman JL. Influence of pulse sequence parameters at 1.5 T and 3.0 T on MRI artefacts produced by metal-ceramic restorations. *Dentomaxillofac Radiol* 2015; **44**: 20150136. doi: https://doi.org/10.1259/dmfr.20150136
34. Hak DJ, Mauffrey C, Seligson D, Lindeque B. Use of carbon-fiber-reinforced composite implants in orthopedic surgery. *Orthopedics* 2014; **37**: 825–30. doi: https://doi.org/10.3928/01477447-20141124-05
35. Kuusisto N, Vallittu PK, Lassila LV, Huumonen S. Evaluation of intensity of artefacts in CBCT by radio-opacity of composite simulation models of implants in vitro. *Dentomaxillofac Radiol* 2015; **44**: 20140157. doi: https://doi.org/10.1259/dmfr.20140157